Journal of King Saud University – Engineering Sciences (2026) 38:39
https://doi.org/10.1007/s44444-026-00114-1

RESEARCH

Vehicle shape influence on virtual forward simulation of car crashes

Michelangelo-Santo Gulino[1] · Giulio Vichi[1] · Gianmarco Aiazzi[1] · Dario Vangi[1]

Received: 2 December 2025 / Accepted: 17 May 2026

Abstract
Progressive deployment of active safety systems requires precise tools to assess collision mitigation performance. Virtual Forward Simulation (VFS) plays a pivotal role in the prospective assessment of Advanced Driver Assistance Systems (ADAS). Reliable VFS routines depend on validated models capable of resolving collision mechanics, particularly when ADAS interventions fail to avoid a collision and the focus shifts to evaluating impact mitigation. However, software tools often omit exact vehicle geometries in accident reconstruction practice. Consequently, when graphical data is compiled for detailed accident records, specifically in the Pre-Crash Matrix (PCM) format, vehicle shapes are typically simplified. Although encoding realistic vehicle shapes demands substantial technical effort during database compilation, this study demonstrates that such fidelity is essential for ensuring high-fidelity outcomes. Data fidelity requirements are identified by investigating the influence of vehicle shape on the reliability of 2D car-to-car collision simulations. A validated tool based on a Reduced Order Dynamic Model (RODM) was used to simulate road collisions using progressively simplified vehicle geometries. Simulations were statistically analyzed and verified through a real-world case study. Findings indicate that while simpler momentum-based models remain insensitive to geometric variations, advanced models like RODM require detailed shapes to accurately resolve impact dynamics. Neglecting this leads to a significant underestimation of key parameters, specifically ΔV (by more than 5 km/h) and occupant injury risk (by up to 60% in real-world scenarios). By defining these data fidelity requirements, this work provides a methodological framework to bridge the gap between current database standards and high-fidelity virtual safety research.

Keywords Virtual forward simulation · ADAS assessment · Accident reconstruction · Vehicle geometry · Delta-V · Injury risk

1 Introduction

In the last 30 years, road traffic injuries have become a major global health issue and a leading cause of non-biological death (World Health Organization 2023). This evidence has prompted the development of structured safety strategies involving both public institutions and the automotive industry. After Sweden's "Vision Zero" in 1997 (European Climate, Infrastructure and Environment Executive Agency 2022), similar programs were adopted globally (Canadian Council of Motor Transport Administrators 2016; Transport for NSW 2022; Organisation for Economic Co-operation and Development 2016, including the EU's goal of zero fatalities by 2050 (European Commission 2003). More recently, several countries have expanded these initiatives by leveraging intelligent transportation systems and big data analysis to improve road safety through smart infrastructure and advanced monitoring (General Authority for Roads, Ministry of Transport and Logistic Services, Saudi Arabia 2025; Roads & Transport Authority RTA, Dubai 2021; National Traffic Safety Committee & Qatar Transportation and Traffic Safety Center 2012.

In parallel, the automotive industry has also reduced road injuries by introducing advanced passive safety systems. All

✉ Giulio Vichi
giulio.vichi1@unifi.it

Michelangelo-Santo Gulino
michelangelosanto.gulino@unifi.it

Gianmarco Aiazzi
gianmarco.aiazzi@edu.unifi.it

Dario Vangi
dario.vangi@unifi.it

[1] Department of Industrial Engineering, University of Florence, Florence, Italy

Published online: 01 June 2026

new passenger cars are equipped with traditional safety systems, such as seat belts, airbags, and survival cell structures, as well as more recent features such as controlled steering column collapse systems (Gotoh et al. 1992) and pedestrian airbags (Hu et al. 2020). Today, a central role in road injury reduction is primarily played by active safety systems such as Anti-lock Braking System, Traction Control System, Electronic Stability Control, and, more broadly, Advanced Driver Assistance Systems (ADAS). The increasing impact of ADAS is confirmed by their progressive mandatory adoption: Autonomous Emergency Braking (AEB) and Lane Keeping Assist (LKA) were made mandatory in 2019 for all new cars type-approved in Europe under the EU General Safety Regulation 2019/2144[1]. According to (Sander and Lubbe 2018), full market penetration of AEB could reduce intersection collisions by up to 79% and lower injuries with a Maximum Abbreviated Injury Scale of at least 2 (MAIS 2+) by 90%. Similarly (Tan et al. 2020), showed that 100% LKA penetration could improve the avoidability of lane-departure collisions, potentially reducing fatalities and injuries by 15 and 10%, respectively.

The performance of safety and injury mitigation systems can be assessed using both *a posteriori* approaches—i.e., when the system under evaluation is already present in a large share of the circulating vehicle fleet—and a priori approaches—i.e., when evaluations are performed before the system is marketed or widely deployed (Alvarez et al. 2017; Gulino et al. 2022). Retrospective (*a posteriori*) analyses rely on real-world accident data, while prospective (a priori) analyses can be supported by real-world pre-crash data and can also be based on test data (driving simulator studies, field operational tests, naturalistic driving studies) or simulations (Virtual Forward Simulation – VFS). In both approaches, the availability of high-quality in-depth accident databases is essential, and evaluation robustness depends on the accuracy and consistency of the database data (Imprialou and Quddus 2019). To ensure correct and representative coding of real-world crashes, advanced mathematical models are required to faithfully reconstruct crash dynamics. These models, implemented in special-purpose software, are crucial in the simulation and reconstruction of road impacts between two or more vehicles, directly influencing the results.

The emphasis on modeling accuracy is supported by research establishing that vehicle geometry and type are primary determinants of crash outcomes. For instance, epidemiological analyses of U.S. crash data have shown that the type of opponent vehicle significantly influences fatality risk; collisions involving buses or heavy trucks can quadruple the fatality risk for powered two-wheeler (PTW) riders compared to passenger vehicles (Terranova et al. 2026). Furthermore, numerical simulations of car–PTW impacts have demonstrated that specific front-end design parameters, such as bonnet leading edge height and length, directly influence head injury risk (IR) (Xiao et al. 2020). Similar correlations have been quantified in pedestrian accidents using in-depth data, where bumper geometry and bonnet heights were found to be statistically significant factors in leg and pelvis IR (Li et al. 2017). These findings underscore that vehicle shape is a critical factor in injury mitigation.

The reconstruction—and therefore the simulation—of the impact phase between two passenger cars can be performed through Finite Element Analysis (FEA) and Multi-Body System (MBS) methods. FEA provides detailed structural results but requires significant computational resources, even considering recent efforts toward more efficient reconstruction methodologies (Costa et al. 2022). Conversely, MBS enables faster dynamic simulations of vehicle interactions, albeit with less structural detail. At the lowest level of complexity, computationally very light but markedly less accurate approaches can be employed, such as momentum-based models, which allow extremely rapid simulation execution (e.g., the method adopted by the Vehicle Safety Institute of Graz University of Technology (TUG) (Kolk et al. 2017)). However, momentum-based models do not provide complete information on vehicle deformations, nor do they provide information on the forces (accelerations or velocity changes) experienced during the impact phase (Brach 1983; Ishikawa 1993). Reduced Order Dynamic Models (RODMs) offer a good balance between complexity, accuracy, and speed (Vangi et al. 2019), and are effective for crash reconstruction and database generation. The computational efficiency of RODMs enables large-scale VFS involving thousands of collisions. This capability supports automated frameworks designed to estimate crash severity across diverse accident scenarios (Breitlauch et al. 2023). However, the predictive potential of these high-fidelity methodologies is inherently linked to the quality of input data. Specifically, it remains to be determined the extent to which vehicle shape influences the accuracy of impact kinematics and IR estimation, and whether simplified representations—commonly used in current practices—are sufficient for advanced simulation frameworks.

The ISO/TR 21934:2021[2] standard provides important guidelines for prospective ADAS performance evaluation via VFS simulations, proposing a method based on comparing simulations without the technology under evaluation (baseline) and replicated simulations with the system installed on the vehicle, in accordance with the methodology

[1] https://eur-lex.europa.eu/eli/reg/2019/2144/oj/eng

[2] Road vehicles—Prospective safety performance assessment of pre-crash technology by virtual simulation.

identified by the P.E.A.R.S. consortium[3] (Page et al. 2015). VFSs aimed at ADAS performance evaluation can be conducted in standard impact configurations or can replicate real-world crashes relying on databases. If the baseline is based on simulations of real-world crashes, VFS requires numerical information on the pre-crash phase from special-purpose accident reconstructions or from in-depth accident databases. In this regard, four of the most established accident databases—namely the GIDAS database (Schubert et al. 2017), IGLAD database (Spitzhüttl et al. 2015), CIDAS database (Shaikh et al. 2024), and RASSI database (Shaikh and Sander 2018)—numerically represent crash scenarios and pre-impact event dynamics in the Pre-Crash Matrix (PCM) format. The PCM format includes information on possible obstacles, traffic signs, buildings, road structures, as well as details on vehicle positions, speeds, and accelerations in the moments preceding the crash (often up to 5 seconds before), allowing a truthful simulation of how the crash actually occurred in the real world. PCM datasets generally provide all the necessary information to simulate a crash using RODM or momentum-based techniques, including vehicle dimensions, inertial properties, and shapes. However, vehicle shapes are encoded in simplified representations; for example, in the IGLAD PCM dataset, vehicles are represented as parallelepipeds or polyhedra with fewer than 10 faces in three dimensions. To date, no study has assessed the feasibility of simplifying detailed vehicle geometries for VFS based on PCM data, nor has any quantified the potential loss of accuracy resulting from this simplification. Filling this gap is critical, as the application of VFS expands from simple collision avoidance to the detailed assessment of collision mitigation during unavoidable impacts, where precise interaction between vehicle structures is paramount.

This work aims to investigate the influence of vehicle shape on the results of car-to-car collision simulations, exploring both the implications for occupant safety assessment in VFS simulations and the effects on impact reconstruction. Specifically, it examines the effect of simplifying the actual shapes of cars on the results of RODM simulations, offering critical insights into the data fidelity levels needed to ensure that virtual assessments accurately reflect collision dynamics and the resulting IR. This analysis was carried out using a dedicated tool for virtual forward simulations and ADAS performance assessment (Gulino et al. 2025), based on a 2D RODM (Vangi et al. 2019) previously validated on 47 real-world crash cases and crash tests. A total of 4320 simulations were performed in standard configurations, varying the shape of one or both cars, and the results were compared in terms ofvehicle velocity change during the impact (ΔV) and deformation energy. Errors on IR were assessed using a ΔV-based Injury Risk Function (IRF) widely used in the literature. Additionally, some simulations in standard configurations were repeated using a momentum-based model, and the results were complemented by a case study on real collisions from the IGLAD PCM dataset, simulating the accidents both with the simplified shapes encoded in the dataset and with actual vehicle shapes.

[3] P.E.A.R.S. is an open consortium (established in 2012 as Harmonization Group) in which engineers and researchers from the automotive industry, research institutes and academia join with the objective to develop a comprehensible, reliable, transparent, and accepted methodology for quantitative assessment of crash avoidance technology by virtual simulation.

2 Materials and methods

To investigate the influence of vehicle shape in VFS simulations, a series of simulations were carried out in standard impact configurations, progressively simplifying the shapes of the vehicles involved. The simulations were performed using a validated special-purpose software tool for simulating road collisions between two passenger cars, based on a 2D RODM.

2.1 RODM-based special-purpose simulation tool

The special-purpose VFS software used in this work implements the RODM algorithms proposed by Vangi et al. (2019) and allows two-dimensional simulation and solution of the impact phase of a road conflict involving two or more participants. This modeling framework is applicable to any collision where three-dimensional effects such as rollover, significant pitch and roll dynamics, or road user projection are negligible. The RODM is fast like momentum-based models but more accurate Le Guennec et al. 2018; Taichi Shiiba et al. 2012; Hamza and Saitou 2005; Pahlavani and Marzbanrad 2015; Witold Pawlus et al. 2011, with ΔV errors generally below 3 km/h. The RODM implemented in the simulation software has been validated in 47 real-world accidents and crash tests (42 cases in (Gulino et al. 2025) and 5 cases in (Vangi et al. 2019)), with each case supported by real crash videos and expert reconstructions to ensure the accuracy of the model validation. Notably, this validation process considered both velocity-based parameters, such as ΔV, and energy-based parameters, specifically the resulting deformed shapes of the vehicles, confirming the model's capability to accurately represent both impact kinematics and energy absorption. The RODM algorithms implemented in this VFS software can be summarized into three distinct modules: "Simulation Initialization," "Vehicle Motion," and "Impact Phase Solution." The individual steps of the simulation are outlined below.

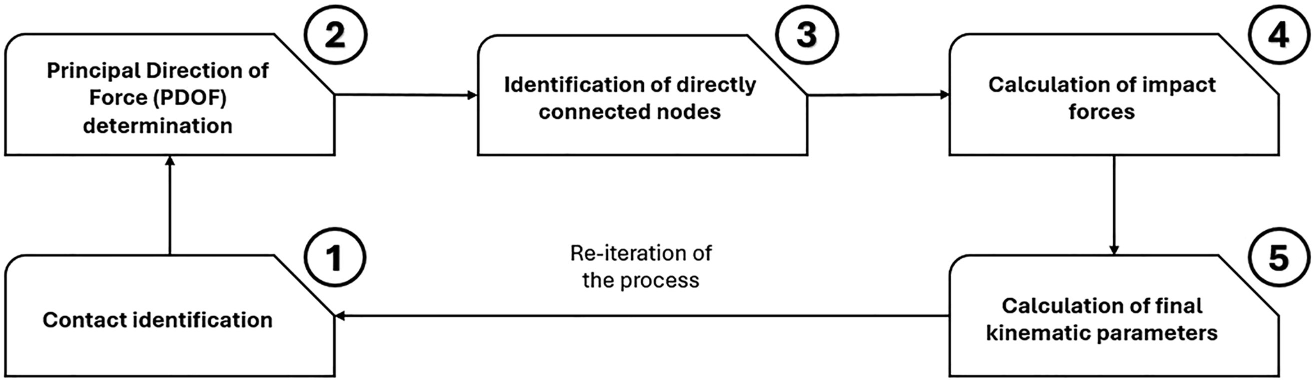

Fig. 1 Algorithm of the "impact phase solution"

Each simulation is initialized by generating each vehicle from a 2D CAD model ("Simulation Initialization"). The external contour of the imported model is discretized into 200 nodes. Each node is connected via spring elements to a virtual reference body that concentrates all the inertial properties of the vehicle. The spring elements model the elasto-plastic behavior of the vehicle as purely elastic (Campbell model (Campbell 1974)). Each spring element is characterized by a specific stiffness value (frontal, lateral, or rear), which can be obtained by analyzing the load–deformation curves from crash tests of the vehicle of interest (McHenry and McHenry 1997; Kubiak 2017). To avoid discontinuities in the distribution of stiffness values, the intermediate nodes between the lateral and frontal or rear zones are assigned intermediate values. In addition, the nodes are sequentially connected to each other through rod elements (no bending moment).

Initialization of each VFS requires setting the initial position of the two generated vehicles and defining the initial conditions in terms of speed (longitudinal velocity and angular velocity), as well as any initial braking and steering inputs. The simulation update time step is set to 5 ms, which is sufficiently small for the specific application field (Le Guennec et al. 2018). Updating the kinematic parameters at each time step enables the vehicles' motion in the virtual environment ("Vehicle Motion").

The "Impact Phase Solution" is comprehensively described in (Vangi et al. 2019) and, for each time step, can be summarized in the five stages illustrated in the diagram of Fig. 1: "Contact Identification" (detection of overlapping nodes of one vehicle within the nodal contour of the other), "Principal Direction of Force (PDOF) determination" (calculation of the direction of locally exchanged forces), "Identification of directly connected nodes" (identification of nodes of the two vehicle contours that mutually exchange impact forces), "Calculation of impact forces" (computation of the forces actually exchanged during the impact), and "Calculation of final kinematic parameters" (updating of the kinematic parameters).

Table 1 Specifications of the vehicles selected for each automotive segment

SEGMENT	MASS [kg]	LENGTH [m]	WIDTH [m]	WHEEL-BASE [m]
A	840	3.54	1.59	2.3
B	1395	4.1	1.99	2.6
C	1190	4.19	1.78	2.57
D	1495	4.62	1.81	2.81
E	1776	4.96	1.88	2.91
SUV	1760	4.84	1.86	2.82

This algorithm is iterated at each time step following the initial contact between the two vehicles until such a time as the separation of the two vehicles is achieved and the impact is concluded. It is important to note that the calculation procedure for the impact forces is applied consistently during both the compression and restitution phases (Vangi et al. 2019); consequently, the restitution behavior is a resulting output of the simulated impact dynamics rather than a predefined input parameter. The algorithm then continues to update the vehicles' kinematic parameters in the same way as during the pre-impact phase, until both vehicles reach rest and the simulation is terminated.

2.2 Simulations in standard configurations

The vehicles used for the simulations were selected to represent the main automotive car segments available on the market, according to the European classification (European Parliament and Council of the European Union 2007). For each segment (A, B, C, D, E, SUV), one of the most commercially widespread vehicles was chosen from those available in an internal database accessible to the authors. Table 1 presents the main characteristics of the vehicles identified for each automotive segment.

The selected vehicle for the B-segment has a curb weight (1395 kg) corresponding to the average mass of the

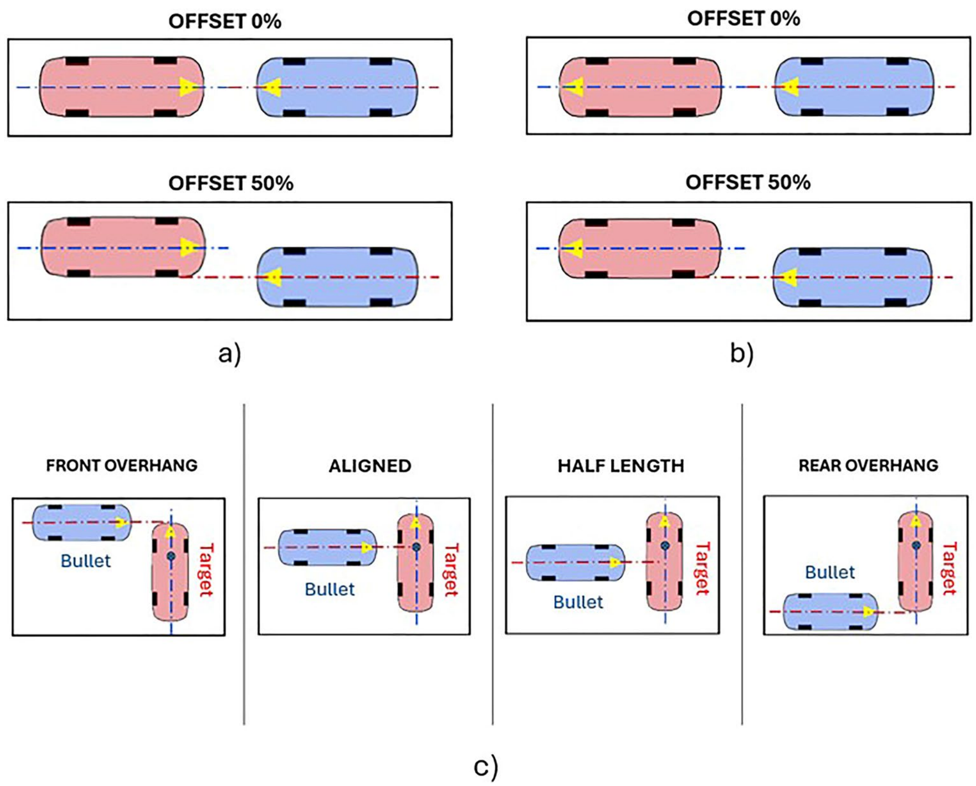

Fig. 2 Front-to-Front (**a**), Front-to-Rear (**b**), and Front-to-Side (**c**) impact configurations adopted in the simulations (in accordance with ISO 6813)

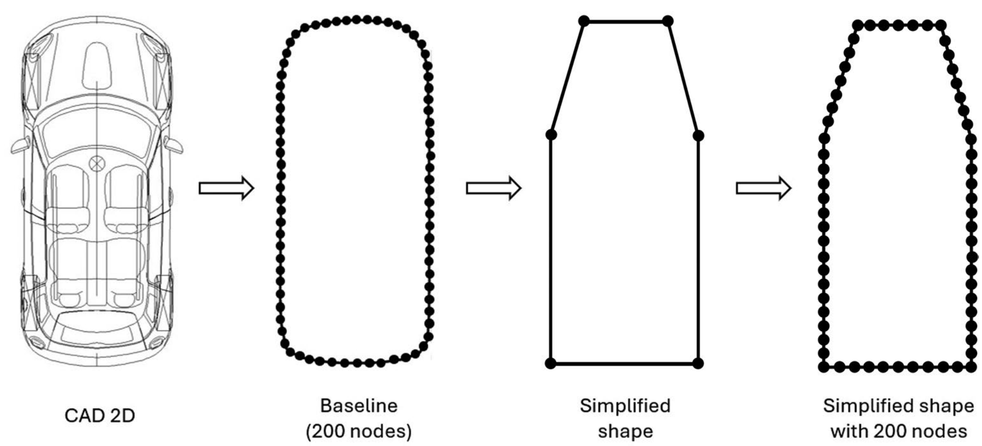

Fig. 3 Representation of the vehicle shape simplification process: from the 2D CAD model to a simplified shape with 6 shape points, but still discretised into 200 nodes

passenger car fleet circulating in Europe in 2018 (Bieker et al. 2019). To avoid overlapping effects on the results due to the simultaneous variation of vehicle mass and geometry, all simulations employ the same vehicle model as both target and bullet, characterized by identical mass and belonging to the same automotive segment.

A total of eight impact configurations were considered in the simulations: two involving Front-to-Front collisions (Fig. 2a), two involving Front-to-Rear collisions (Fig. 2b), and four involving Front-to-Side collisions (Fig. 2c). The adopted Front-to-Front and Front-to-Rear configurations are distinguished between centered impacts (0% offset) and impacts with eccentricity (50% offset). The Front-to-Side configurations were selected with four different offsets so that the target vehicle is impacted at different positions along its left side: near the center of mass (Aligned), the passenger compartment (Half Length), and the front and rear overhangs (Front Overhang and Rear Overhang).

Each simulation was conducted with the target vehicle velocity set to zero and the bullet vehicle velocity set to three different impact speeds, 30, 50, and 90 km/h, in accordance with the main speed limits in urban and extra-urban scenarios. The 120 simulations performed (5 segments, 8 impact configurations, 3 impact speeds) were replicated by gradually simplifying the shape of the vehicles used. Node decimation was applied starting from the 200 nodes defining the vehicle perimeter in the simulation environment (baseline), as shown in Fig. 3. The choice of 200 nodes for the baseline

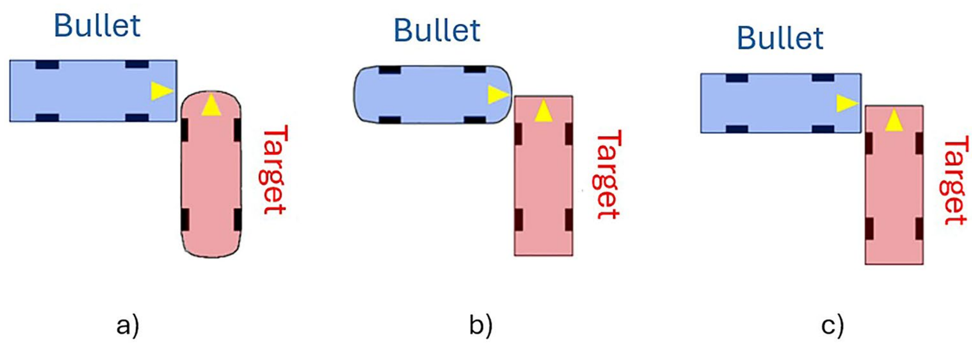

Fig. 4 Example of simplification of the bullet vehicle (**a**), target (**b**) or both simultaneously (**c**)

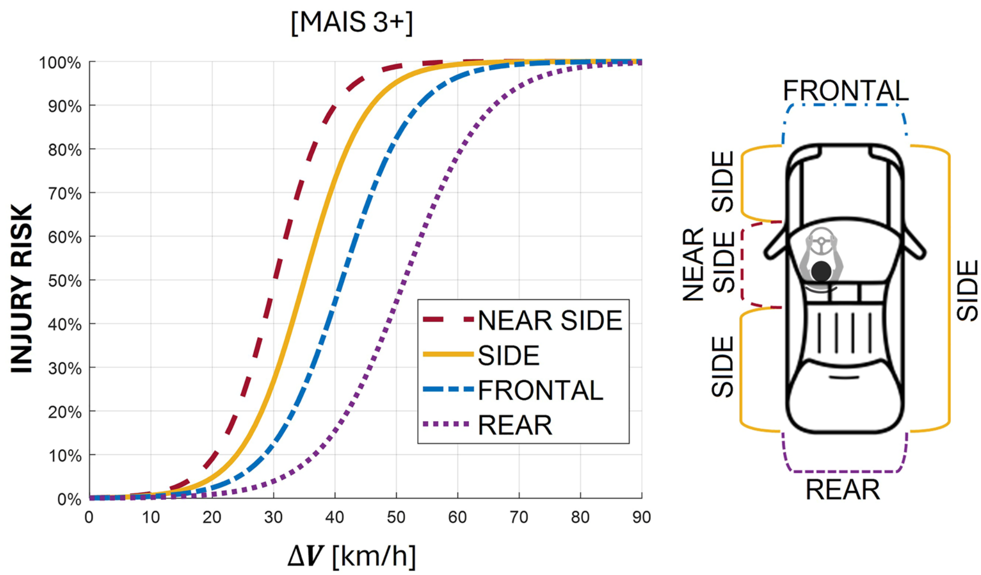

Fig. 5 IRF adopted

was adopted to ensure a robust representation, as literature indicates that, when employing this type of RODM, 50 nodes are typically sufficient to satisfactorily describe the impact behavior of a vehicle (Vangi et al. 2019). Specifically, the simulation tool used in this work was previously validated across different automotive segments using this exact configuration of 200 nodes (Gulino et al. 2025). For each of the six vehicles employed, 11 simplified vehicles were obtained, defined respectively by 150, 100, 50, 40, 30, 20, 15, 10, 8, 6, and 4 nodes (shape points). By connecting the shape points, eleven simplified perimeters are generated. The collision detection algorithm of the simulation software is based on the overlap of a vehicle's nodes within the nodal contour of the other vehicle. Therefore, to ensure that the simulation software can always detect the intrusion of one vehicle's nodes into the other, 200 nodes are regenerated on each simplified perimeter. This ensures that the simulation software can consistently and accurately detect the intrusion between two vehicles during impact.

A total of 4320 simulations were performed: the simplified shapes were first applied to the bullet vehicle (Fig. 4a), then to the target vehicle (Fig. 4b), and finally to both vehicles simultaneously (Fig. 4c). Each simulation produced two post-crash outputs. The first output is the ΔV of the target vehicle, which is a kinematic parameter. The second output is an energy-related parameter, defined as the sum of the maximum deformation energy of the two vehicles.

Furthermore, for each simulation, IR of the drivers involved in the collision was evaluated using the IRF proposed by (Jurewicz et al. 2016), which was selected because it accounts for the impacted vehicle area by distinguishing between four distinct zones, thus indirectly incorporating the influence of vehicle crush and structural response based on the impact configuration. The IRF employed relates the ΔV and the impacted vehicle area to the probability that the driver of the struck vehicle sustains severe injuries (MAIS3+), as shown in Fig. 5. The adoption of these curves assumes that occupants are correctly restrained by seatbelts, vehicles are equipped with airbags, and the collision is limited to a primary impact without rollover or secondary impacts.

The results obtained from each simulation conducted under the standard configurations of Fig. 2 (with at least one of the two vehicles simplified) were compared with the results of the corresponding simulation carried out with the actual vehicle shapes (baseline). The ΔV, total deformation energy, and IR from the simulations with simplified shapes were therefore expressed as errors relative to the corresponding outputs of the baseline.

2.3 Case study

In addition to the simulations previously described, the influence of vehicle shape in VFS simulations was further investigated by performing 20 additional simulations based on real-world accidents. For this purpose, the IGLAD PCM database was used. This database contains real crash cases in which the accident scenario and event dynamics (up to the first contact between the two vehicles) are numerically encoded. The information provided allows the accidents to be accurately reproduced in simulation, offering highly detailed data regarding the impact configuration (vehicle heading, offset, relative speed, etc.) (Spitzhüttl et al. 2015).

Figure 6 shows an example of a PCM used, including, for illustration purposes, information on the positions of the bullet and target vehicles at different Time-To-Collision (TTC) values.

The IGLAD PCM database does not provide detailed information on vehicle shapes; in 2D plan view, vehicles are coded as rectangles (4 shape points) or rectangles with one of the shorter sides chamfered (6 shape points). No information on the stiffness of the coded vehicles is available. Therefore, the 20 car-to-car collision cases were selected based on the availability of 2D CAD models and stiffness data for the vehicles involved in the conflicts. This allowed the 20 PCM cases to be simulated using the special-purpose simulation tool described in Sect. 2.1.

A consistency check of the kinematic data for the selected cases was performed based on momentum conservation and the compatibility between pre- and post-impact velocities, using both the post-crash information coded in the IGLAD database and the pre-crash data from the PCM dataset, following the procedure indicated by (Vangi et al. 2019).

Table A1 in the Appendix reports, for each selected accident, the vehicles involved, their impact configuration, and the respective ΔV values (baseline coinciding with the database values). The 20 identified PCM cases all involve vehicles coded as rectangles. Each PCM case was first simulated with the actual 2D vehicle shapes, and then with the two vehicles represented as rectangles (4 shape points), as coded in the database. Stiffness values, as well as parameters encoded in the PCM database (e.g., vehicle masses), were kept unchanged in both simulations.

The outputs of each simulation were used to calculate the IR of the driver of each vehicle, again using the IRF proposed by (Jurewicz et al. 2016). In total, 9 real-world Front-to-Side accidents, 4 Front-to-Rear accidents, 3 Sliding accidents, 2 Front-to-Front accidents, and 2 Small Overlap (frontal) accidents were simulated.

3 Results

For each of the six automotive segments identified, eight standard impact configurations were simulated at three different collision speeds of the bullet vehicle, resulting in a total of 24 scenarios. The influence of shape simplification on ΔV, deformation energy, and IR of the target vehicle was therefore investigated across the 24 scenarios for each of the six automotive segments considered.

Figure 7 illustrates, as an example, the trend of the target vehicle's ΔV as a function of the shape simplification (shape points) of the bullet vehicle only, in the "Half Length" configuration with a bullet collision speed of 90 km/h. A shape

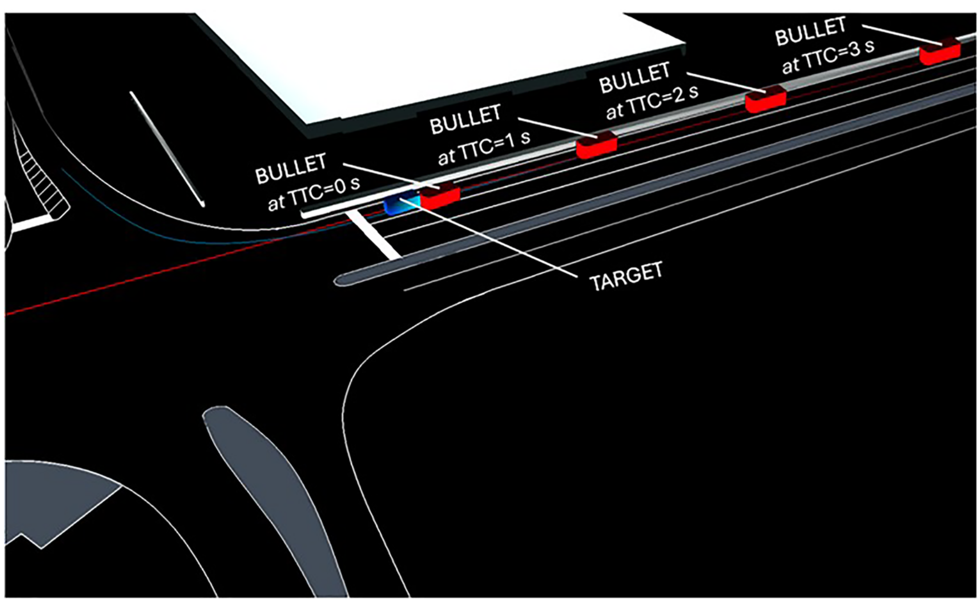

Fig. 6 Graphical representation of an IGLAD PCM. Bullets and targets are represented at different TTC

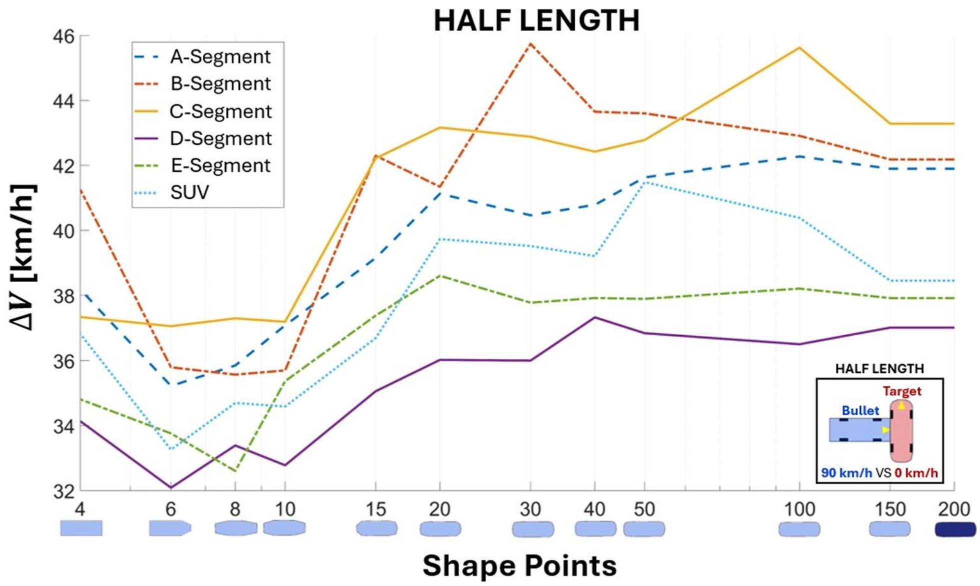

Fig. 7 Trend of the target vehicle's ΔV as a function of the number of shape points of the bullet vehicle for the six automotive segments considered in the "Half Length" scenario with a relative velocity of 90 km/h

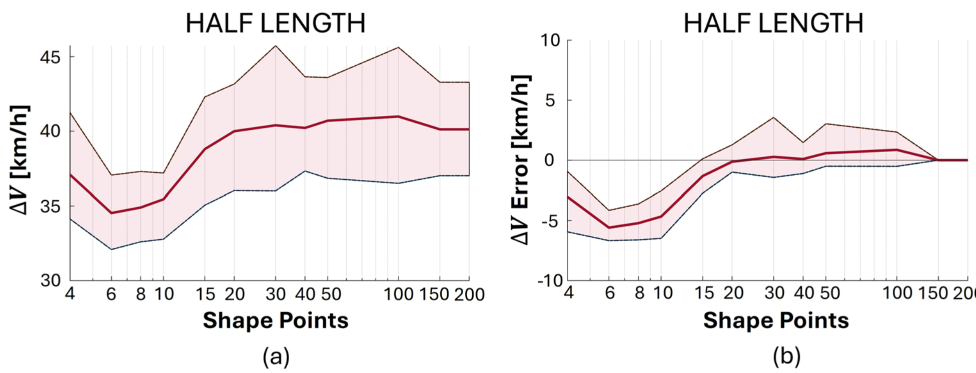

Fig. 8 Average trend and confidence intervals of ΔV (**a**), and trend of the ΔV error (**b**), in the "Half Length" scenario with bullet vehicle speed equal to 90 km/h

point value of 200 corresponds to the 2D CAD representation of the actual vehicle; this condition is regarded as the reference associated with the true values of ΔV, deformation energy, and IR, thus serving as the baseline for evaluating the errors introduced by vehicle shape simplification.

When each segment is considered individually, Fig. 7 shows that the largest variability of the target's ΔV with respect to bullet shape occurs in the B-segment (10 km/h, between 8 and 30 shape points). In a single collision involving a bullet and a target of the same segment, both vehicles share the same mass and therefore the same ΔV (by conservation of momentum). The differences in ΔV among bullet vehicles from different segments, when 200 nodes are used, are instead attributable to the distinct frontal stiffness of each vehicle.

The ΔV trends of each segment (target) were averaged (Fig. 8a) and expressed as absolute errors with respect to the baseline mean value (Fig. 8b), corresponding to the same scenario as in Fig. 7. Fig. 8 shows the envelope of the values, accounting for the variability resulting from the use of different segments as bullet vehicles. Considering all segments, Fig. 8b indicates that the error relative to the baseline can reach up to 6 km/h (at 6 shape points). Moreover, the largest difference among the various segments in the absolute error plot occurs at 4 shape points (rectangular shape, typical in PCM cases), with a value of 5 km/h. Errors become smaller than 3 km/h when the number of shape points exceeds 40.

Similarly, the errors in the average trend of total deformation energy and IR were computed. Figure 9 shows the error in ΔV and in total deformation energy for four Front-to-Side conflict scenarios (Half Length, Aligned, Rear Overhang, and Front Overhang), as a function of the number of shape points of the bullet vehicle impacting the target vehicle at 90 km/h. Although the plots in Fig. 9 do not indicate a particularly clear trend, both the ΔV error and the energy error decrease as the number of shape points increases, i.e., as the geometric detail of the vehicle shape improves. Errors tend to vanish beyond 100 shape points, for both ΔV and deformation energy. In absolute terms, the lowest errors are observed in the "Aligned" configuration.

Similar considerations can be drawn from the error trends reported in the Appendix (Fig. A1–A7), where results for the 90 km/h bullet speed are reported as representative

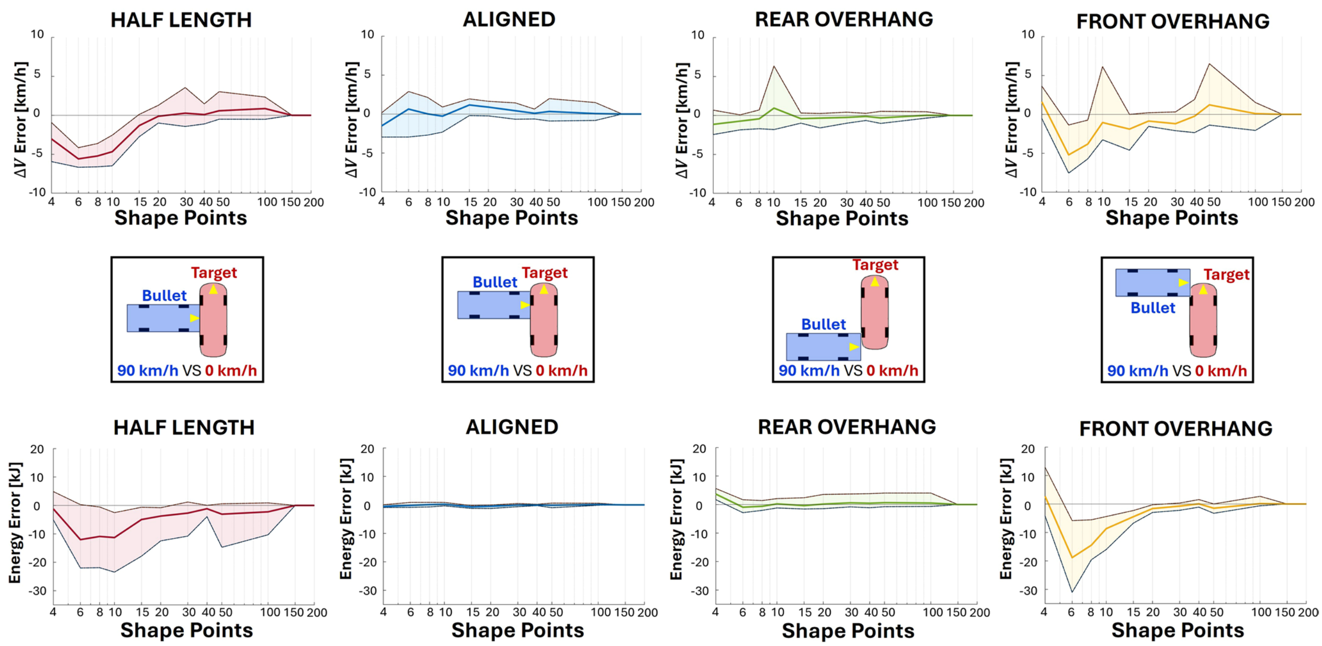

Fig. 9 Trend of the error in ΔV and total deformation energy in the four Front-to-Side scenarios simulated with a bullet vehicle speed of 90 km/h

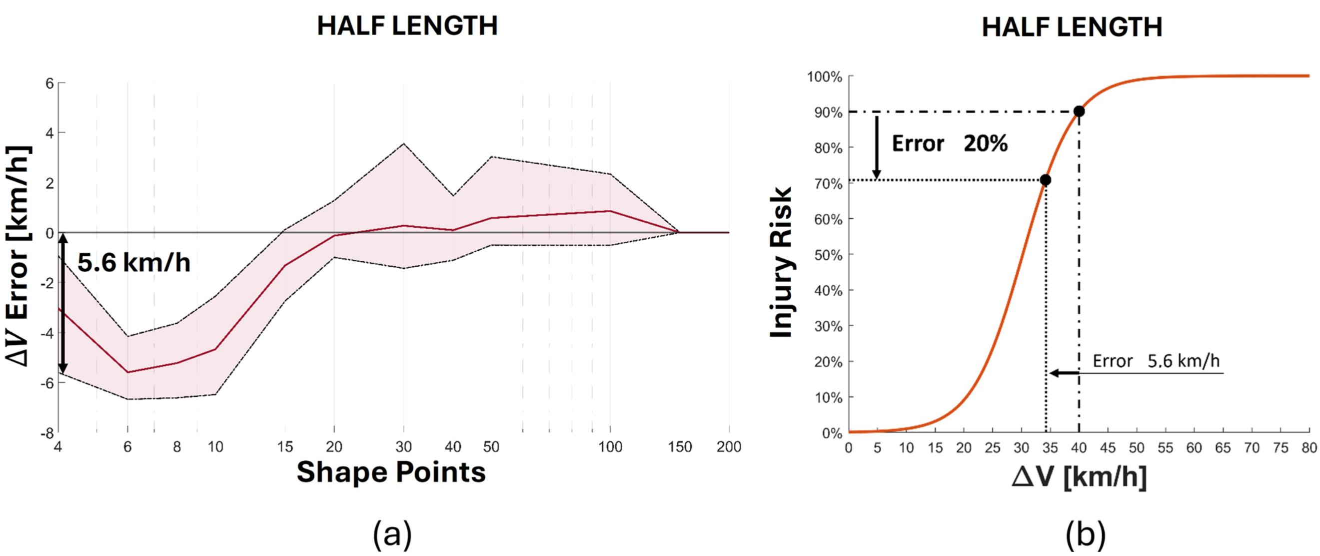

Fig. 10 Error in ΔV (a) and in IR (b) obtained with a rectangular bullet vehicle in the "Half Length" scenario. Bullet velocity equal to 90 km/h

of the general trends observed across all scenarios. The IR values were derived from an IRF (Fig. 5) expressed through logit curves. Similarly, the main IRFs commonly used to evaluate vehicle occupant safety in car-to-car collisions are based on ΔV and are typically represented by logit or probit functions (Gulino et al. 2025). As a consequence, these IRFs exhibit specific intervals characterized by steep slopes, where even small errors in ΔV may lead to large errors in IR. This effect is clearly illustrated in Fig. 10, which refers to the "Half Length" impact scenario with a simplified target vehicle colliding with the bullet vehicle at 90 km/h. Fig. 10 shows that, with the IRF used, an error in ΔV of 5.6 km/h—caused by adopting the rectangular vehicle shape (4 shape points)—may result in an underestimation of the driver's absolute IR value from 90% to 70%.

The definition of vehicles as simplified shapes represented by 4 shape points in 2D (or at most 6 shape points) is widespread in accident databases that provide detailed pre-crash information, such as IGLAD PCM. The Appendix reports the results of simulations carried out on the 20 selected

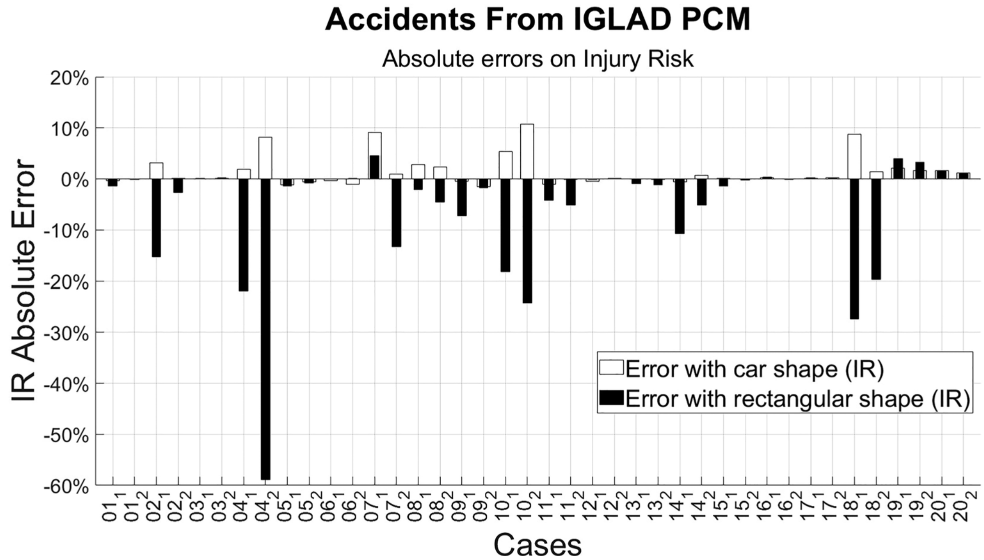

Fig. 11 IR errors obtained by simulating vehicles with their actual shapes (in white) and with rectangular shapes extracted from the database (in black). The errors are expressed relative to the reconstructed values encoded in the IGLAD PCM database. Subscripts distinguish between participant 1 and participant 2 in the same collision

Table 2 Results of the statistical analysis: correlations between the errors (on ΔV, deformation energy, and IR) and the main simulation parameters (impact configuration, collision speed, car segment, shape points, simplified vehicle). Asterisks (*) denote statistically significant p-values ($p < 5\%$)

		Impact configuration	Collision speed	Car segment	Shape points	Simplified vehicle
ΔV Error	Pearson correlation	0.027	0.026	−0.023	−0.197	−0.035
	p-value	6.7%	7.5%	11.6%	0.1%*	1.7%*
Energy Error	Pearson correlation	0.044	0.019	−0.030	−0.142	−0.105
	p-value	2.0%*	18.4%	4.0%*	0.1%*	0.1%*
IR Error	Pearson correlation	0.057	0.094	−0.018	−0.188	−0.043
	p-value	0.1%*	0.1%*	21.0%	0.1%*	0.3%*

PCM cases, validated for data consistency: Table A2 presents the results and errors in terms of ΔV, while Table A3 presents those in terms of IR. The errors obtained from the simulations are expressed as differences relative to the reference values encoded in the database (reconstructed from real crash videos and expert analyses); therefore, even simulations performed with 200 shape points include intrinsic deviations.

For each simulated crash, Fig. 11 shows the IR error relative to the reconstructed database value, using both the actual shapes of the two vehicles and the rectangular shape (4 shape points) as encoded in the database. Errors obtained with the actual vehicle shapes never exceed 11%, whereas those obtained when simulating the vehicles as rectangles reach 20% in three cases, and up to about 60% in a single case. It can thus be inferred that the use of rectangular vehicle shapes tends to underestimate IR, particularly when errors exceed 5% in absolute terms. Conversely, the use of detailed shapes tends to slightly overestimate IR. Similar considerations, though less pronounced, can also be drawn when comparing the errors in ΔV, as highlighted in Fig. A8 in the Appendix, which reports for each participant, the ΔV value encoded in the database and the errors obtained using the actual shape and the rectangular shape.

4 Discussion

We statistically analyzed how errors in ΔV, Energy, and IR relate to impact configuration, collision speed, car segment, vehicle shape, as well as to which vehicle was simplified (bullet, target, or both). Table 2 reports the p-values and Pearson correlation coefficients between each considered error and each simulation parameter: "Impact configuration", "Collision speed", "Car segment", "Shape points", and "Simplified vehicle" (i.e., information on which vehicle was simplified among target, bullet, or both). Strong correlations were observed between all three errors and the parameters "Shape points" and "Simplified vehicle". The p-value related to vehicle shape ("Shape points") is 0.1% for all errors. The correlation coefficients related to vehicle shape are negative; thus, the errors decrease as the level of shape detail increases (i.e., as the number of shape points increases). The parameter "Simplified vehicle" indicates the vehicle undergoing shape simplification, i.e., whether the number of shape points of the bullet, the target, or both simultaneously is reduced. This parameter also has a p-value below 2% for the error on ΔV and below 0.5% for the errors on deformation energy and IR. Overall, the number of shape points and the "Simplified vehicle" can be identified as two influential parameters across all types of errors. The error on deformation energy is also correlated with the impact configuration (p-value equal to 2%), since each impact configuration involves different vehicle nodes and, consequently, different stiffness values that lead to varying deformations and deformation energies. The error on IR is also correlated with the impact configuration as well as with the collision speed, presenting a p-value of 0.1% in both cases. The cause of this correlation lies in the nature of the employed IRF, which depends on ΔV and on the impacted area of the vehicle, as shown in Fig. 5. Specifically, the non-uniform sensitivity of IR errors to ΔV variations stems from the sigmoidal nature of logit risk curves. While minor discrepancies result in disproportionate IR shifts within steeper intervals, the effect is significantly attenuated in flatter regions, particularly at lower initial speeds (e.g., 20 km/h) where the curve gradient is minimal. The magnitude of shape-induced errors is thus intrinsically modulated by the specific ΔV range of the impact, which is strongly dependent on the collision speed (Roberts and Compton 1993), while the impacted vehicle area remains a direct consequence of the impact configuration. The "Car segment" parameter does not show significant correlation with the errors, except for a weak correlation with deformation energy (p-value equal to 4%), despite what can be inferred from Figs. 7 and 8, where significant variability of the results as a function of the car segment is observed.

The statistical analysis of the results of simulations conducted in standard impact configurations shows how vehicle shape simplification affects the results, both in terms of deformation energy and ΔV, and therefore IR. The p-value related to vehicle shape (shape points) is 0.1% for all three considered errors, indicating that the influence of vehicle shape on the errors is statistically significant. The correlation coefficients related to vehicle shape are negative, meaning that the errors decrease as the level of shape detail increases. The "Simplified vehicle" parameter always has a p-value below 2%, highlighting its correlation with the errors. Therefore, to achieve accurate results in 2D VFS simulations, it is essential to employ detailed geometries for both vehicles, as preserving the real shape of only one vehicle proves insufficient for a reliable crash representation.

The simulations carried out in the eight standard configurations (Fig. 2) always use the same vehicle as both target and bullet (even if one or both have simplified shapes), and

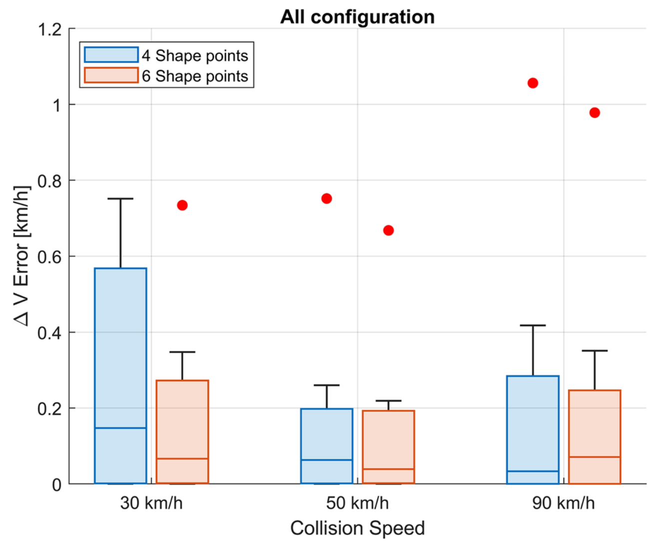

Fig. 12 Boxplot of the ΔV errors from the momentum-based simulations, expressed relative to a simulated baseline obtained with the same simulation model using 200 shape points

the target vehicle always has zero velocity at the time of collision. The results obtained with these two simplifications are sufficient to be generalized, as using different vehicles for bullet and target or a non-zero target collision speed would only lead to greater variability of the results and larger errors. The 20 examples from the PCM case study, where bullet and target are different vehicles each with its own collision speed, show IR errors significantly higher than those obtained in the 4320 simulations with standard configurations. Moreover, the proposed PCM case study also highlights that simulating vehicles with rectangular shapes may lead to a considerable underestimation of the IR for vehicle occupants.

Finally, for completeness and scalability of the analysis, the standard impact configurations shown in Fig. 2 were also simulated using a different impact reconstruction model under the same collision conditions. Collisions between identical segment C vehicles (Table 1) were simulated with the 2D momentum-based impact model developed by TUG (Kolk et al. 2017). The purpose of this additional analysis was not to compare the accuracy of the results obtained with the RODM and the momentum-based model in reproducing ΔV and IR, as this aspect has already been addressed in a previous study (Gulino et al. 2025). Rather, the aim is to investigate whether vehicle shape exerts a comparable influence when using simpler and less accurate simulation models.

The two vehicles were defined with 200 shape points (baseline), 6 shape points (typical PCM shape), and 4 shape points (rectangular shape). The TUG momentum-based model is capable of calculating PDOF, post-crash velocity, and ΔV as output parameters. Figure 12 reports the results expressed as the error on ΔV compared to the simulations with 200 shape points. The errors committed when varying the shape in the momentum-based model are extremely small, ranging from 0 to $1.1\ km/h$. Therefore, the employed momentum-based model is insensitive to shape simplification. However, it is a simplified model compared to the previously used RODM: it does not allow determination of the deformations sustained by the vehicles after the collision, nor the deformation energies (or Energy Equivalent Speed - EES); it only calculates the main kinematic parameters, on which it makes non-negligible estimation errors both for accident reconstruction purposes and for ADAS performance assessment, as highlighted in terms of ΔV error by Smit et al. particularly for sliding impacts (Smit et al. 2019) or by Gulino et al. for all impact configurations (Gulino et al. 2025). For this reason, Fig. 12 shows the internal consistency of the results for simulations with 4, 6, and 200 shape points; it does not reflect the actual ability of the software to provide the real ΔV value through a discretization by 200 shape points.

5 Limitations

While this study provides a comprehensive analysis of vehicle shape influence, certain considerations regarding the IR assessment phase should be noted. The adoption of an approach based on ΔV is supported by its role as a primary, well-established predictor of injury severity. However, the specific IR functions employed do not directly incorporate passenger compartment intrusion, accounting for this factors indirectly through the impacted vehicle area as structural proxies. Furthermore, the analysis assumes the use of standard passive safety features, such as airbags and seatbelts, and focuses exclusively on the driver. Consequently, these results may not be fully generalizable to other occupants whose injury mechanisms are influenced by different seating positions and interior geometries.

Regarding the physical modeling, it should be clarified that while contact parameters such as friction and the inherent variability of vehicle stiffness are integral components of the simulation framework, they were not subjected to a specific sensitivity analysis in this research. The study was intentionally focused on isolating errors stemming exclusively from geometric simplification, although it is acknowledged that the interplay with these physical variables represents a relevant area for future exploration.

It should also be noted that error quantification is performed relative to a numerical baseline rather than direct experimental crash test data for every scenario. However, this baseline is grounded in a model previously validated against real-world collisions and experimental tests, including non-traditional configurations.

Finally, the current framework is inherently two-dimensional, which means it excludes 3D phenomena such as pitch and roll dynamics or override and underride effects. While this planar focus is consistent with the scope of the adopted ΔV-based IRF, which is designed for impact configurations where planar dynamics predominate rather than for complex events such as rollovers, the exclusion of three-dimensional interactions remains a limitation that suggests a natural progression for future research to further improve the fidelity of virtual safety assessments.

6 Conclusions

The guidelines for the prospective evaluation of ADAS safety performance through virtual simulations, provided by ISO/TR 21934, recommend comparing simulations performed without the system under evaluation (baseline) with those repeated with the system installed in the vehicle. Comprehensive assessments of ADAS performance require simulating system intervention in real accidents, which makes the use of detailed pre-crash databases essential. These databases, typically structured in the Pre-Crash Matrix (PCM) format, contain numerical descriptions of the pre-crash phase but usually encode vehicle shapes with simplified two-dimensional rectangles.

This study examined the influence of vehicle shape simplification on car-to-car 2D collision simulations, highlighting the resulting errors in key parameters for impact reconstruction and in Virtual Forward Simulation (VFS) outputs used to estimate Injury Risk (IR).

A validated Reduced Order Dynamic Model (RODM) was used to simulate 24 standard crash scenarios, progressively simplifying the geometry of six vehicles representative of major automotive segments. Statistical analysis of the 4,320 simulations performed under standard configurations revealed clear correlations between the degree of vehicle shape simplification and the errors in ΔV, deformation energy, and IR, relative to the reference values obtained with the actual vehicle geometries.

The results confirm the need for detailed geometries for both vehicles involved in a collision when employing an advanced simulation model, as shape simplification significantly affects IR estimation. In this context, the observed influence of geometry on IR reflects the sensitivity of the ΔV-based IRF within the specific dynamics of the 2D modeling framework, particularly in the steeper intervals of the risk curves where minor velocity variations lead to the largest discrepancies. With the RODM used in this study, a 5 km/h variation in ΔV due to shape simplification can lead to absolute IR errors of up to 25.6% in lateral impacts, 20.7% in frontal impacts, and 18.0% in rear impacts (corresponding to the steepest and most sensitive intervals of the adopted IRF). Conversely, the effect of shape-induced velocity errors is significantly attenuated in the flatter portions of the curves, such as at very low or very high ΔV.

In the analyzed real-world case study based on accidents from the IGLAD PCM database, simplified rectangular vehicle geometries led to a significant underestimation of occupant IR. For example, with the employed IR function, a ΔV error of 15.5 km/h produced an IR deviation of 58.9%. In contrast, the additional simulations conducted with the momentum-based model confirmed that such simplified approaches are insensitive to vehicle shape.

These results show that detailed geometries are needed for reliable ADAS assessment, even if they require more effort. Realistic geometries make data suitable for advanced models and allow accurate estimation of ΔV, energy, and IR. From the dataset user perspective, the influence of vehicle geometry depends on the chosen model: while rectangular representations remain practical for momentum-based approaches, high-accuracy VFS models like RODM require incorporating detailed geometries to ensure that prospective assessments are not compromised by data simplification. This work helps align database standards with high-fidelity virtual safety research. The critical role of vehicle geometry identified in this planar framework suggests that its influence would be even more pronounced in complex 3D environments. Consequently, extending this analysis to three-dimensional impact models represents a natural progression for future research to further improve the fidelity of virtual safety assessments. To support this progression, the adoption of high-fidelity vehicle geometries remains a critical requirement for accurate, robust virtual crash and IR assessments.

Appendix A

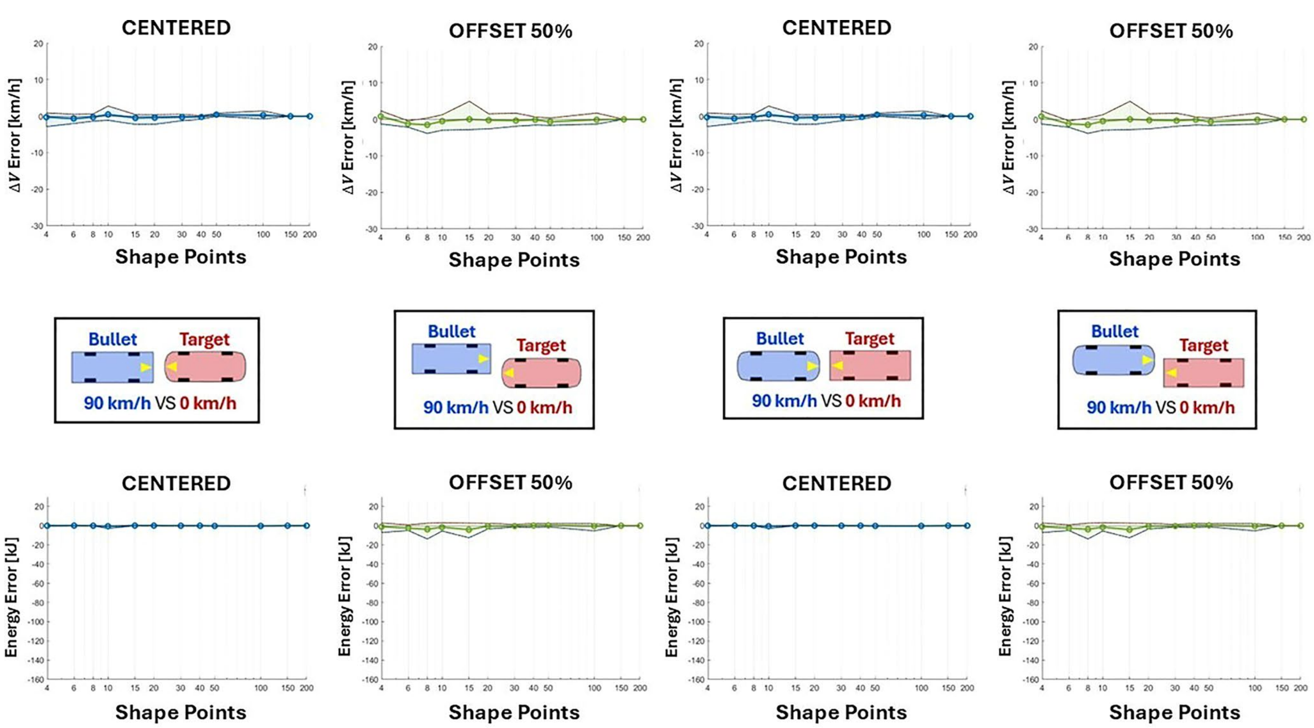

Fig. A1 Trend of the error in ΔV and total deformation energy in the Front-to-Front scenarios simulated with a bullet vehicle speed of 90 km/h (simplification of the bullet shape only and semplification of the target shape only)

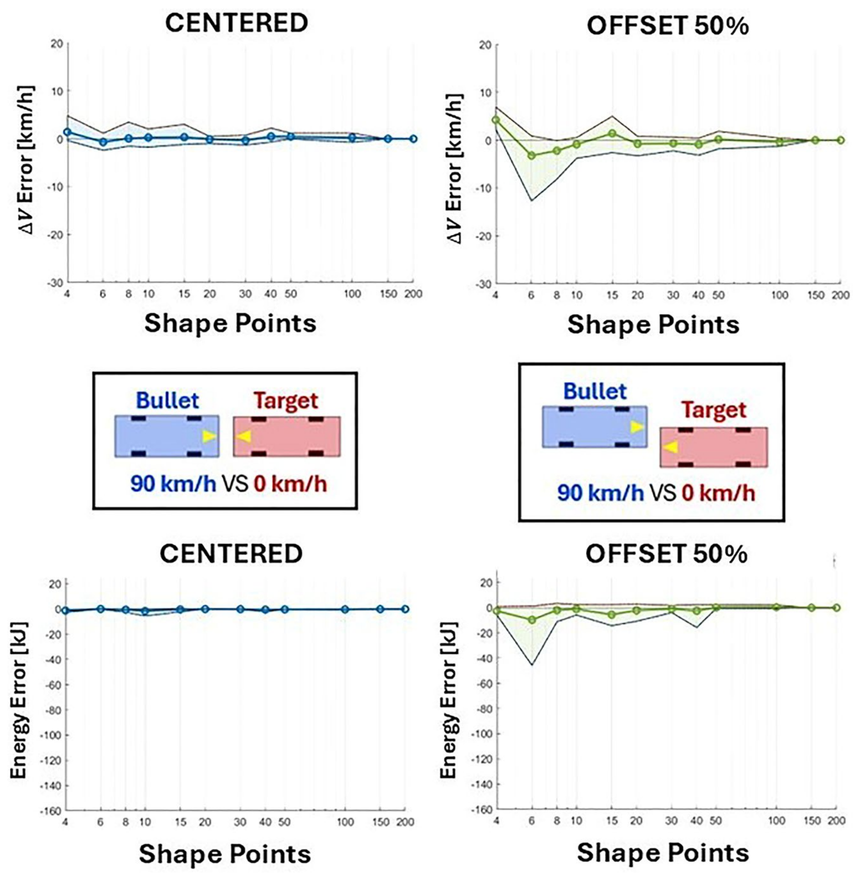

Fig. A2 Trend of the error in ΔV and total deformation energy in the Front-to-Front scenarios simulated with a bullet vehicle speed of 90 km/h (simplification of the shape of both vehicles)

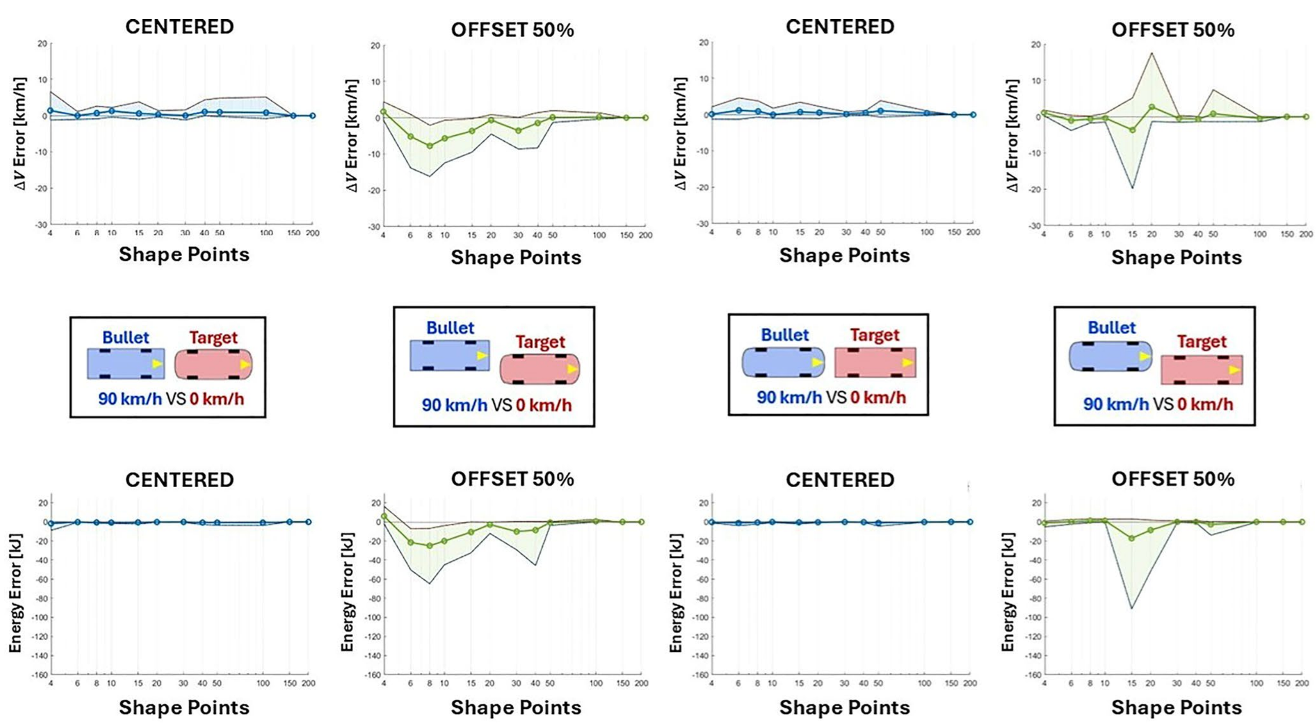

Fig. A3 Trend of the error in ΔV and total deformation energy in the Front-to-Rear scenarios simulated with a bullet vehicle speed of 90 km/h (simplification of the bullet shape only and simplification of the target shape only)

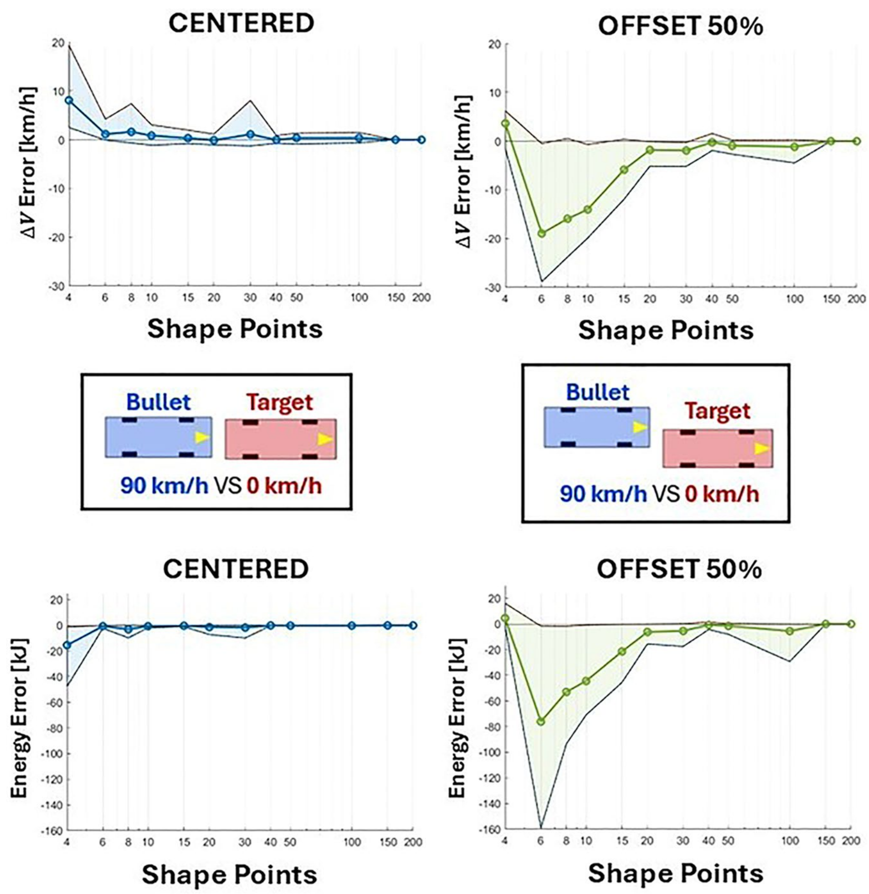

Fig. A4 Trend of the error in ΔV and total deformation energy in the Front-to-Rear scenarios simulated with a bullet vehicle speed of 90 km/h (simplification of the shape of both vehicle)

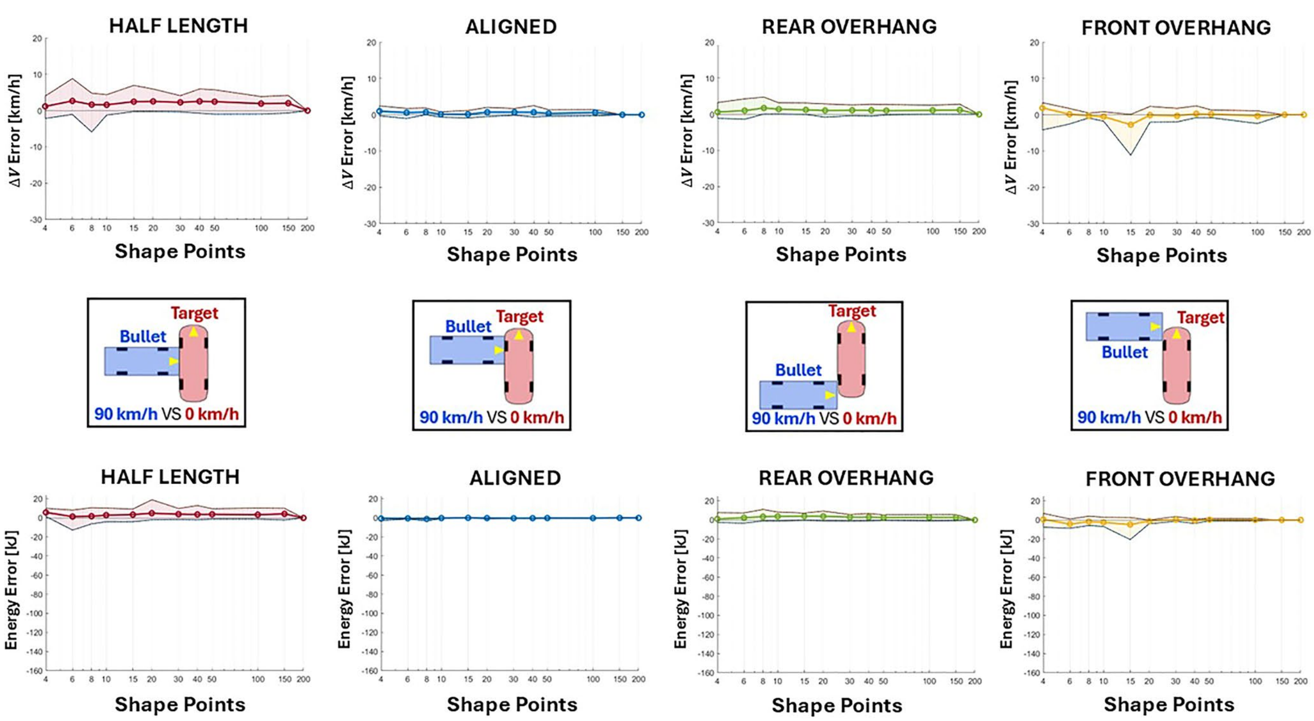

Fig. A5 Trend of the error in ΔV and total deformation energy in the Front-to-Side scenarios simulated with a bullet vehicle speed of 90 km/h (simplification of the bullet shape only)

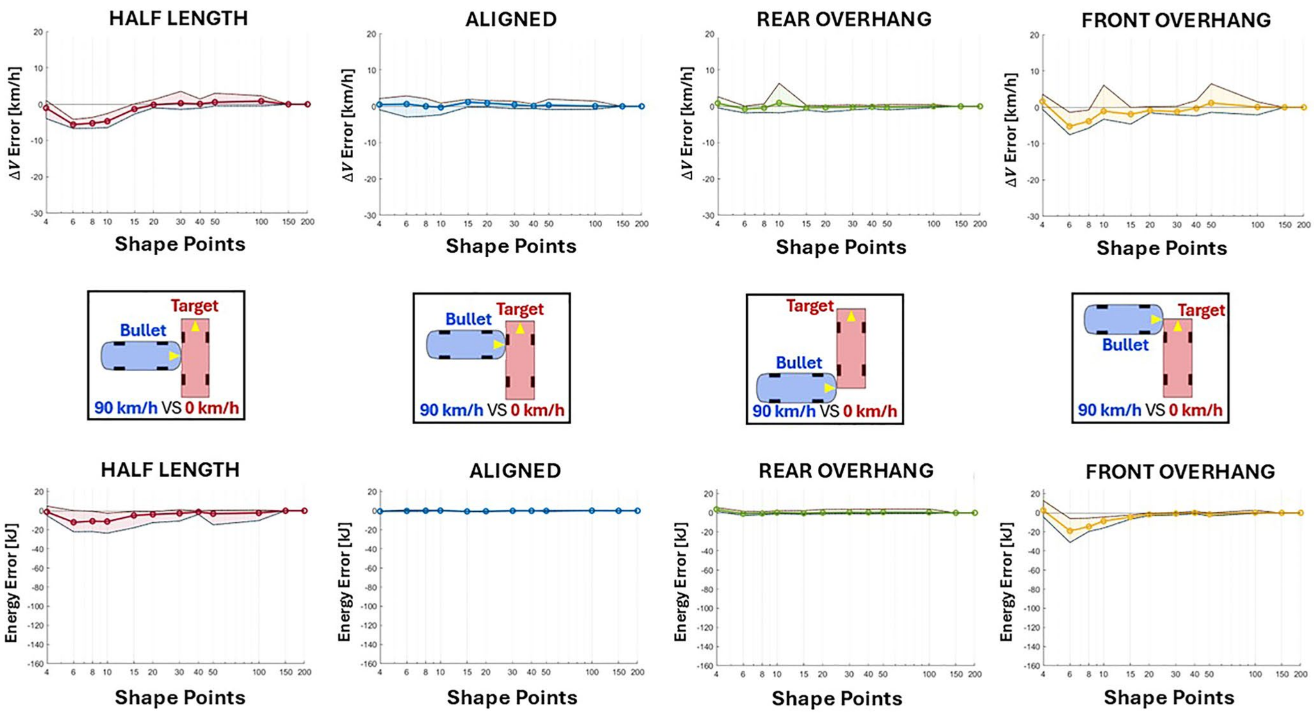

Fig. A6 Trend of the error in ΔV and total deformation energy in the Front-to-Side scenarios simulated with a bullet vehicle speed of 90 km/h (simplification of the target shape only)

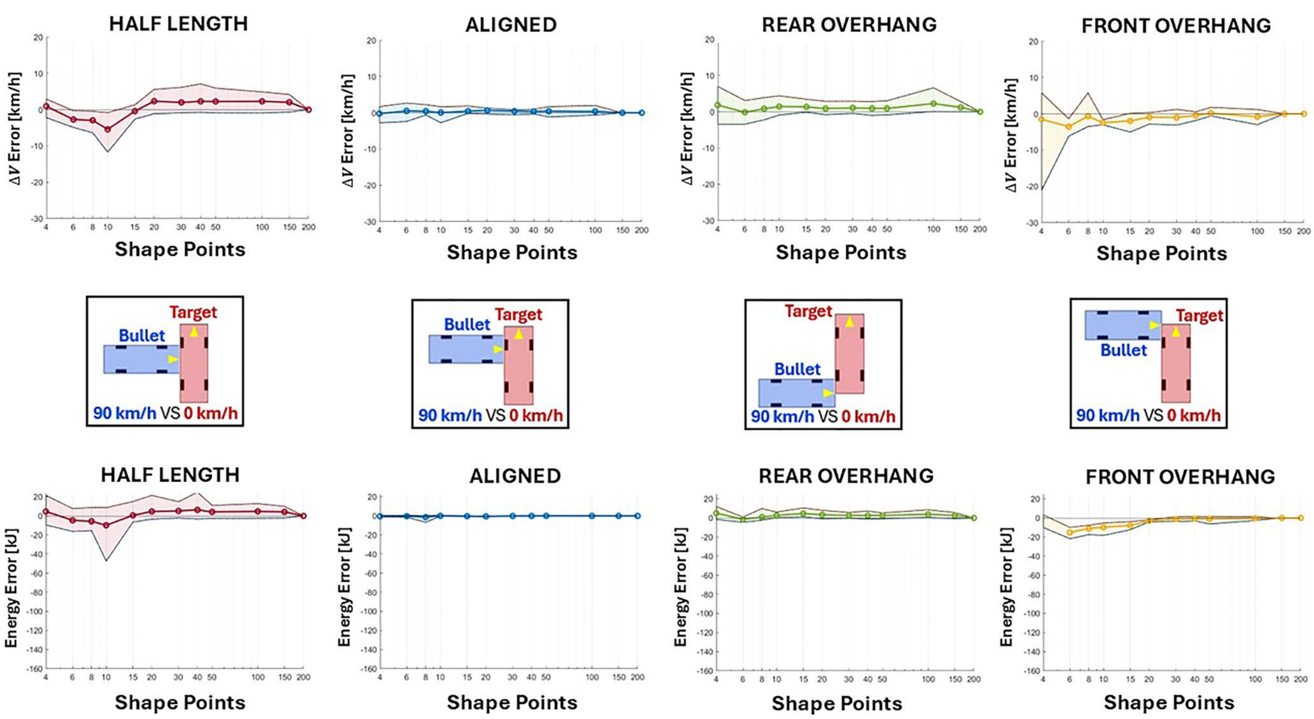

Fig. A7 Trend of the error in ΔV and total deformation energy in the Front-to-Side scenarios simulated with a bullet vehicle speed of 90 km/h (simplification of the shape of both vehicle)

Table A1 Information regarding the 20 real accidents extracted from the IGLAD PCM database. Respectively: accident identifier (ID), participant identifier (PARTNR), impact configuration (TYPE), car segment (SEGMENT), ΔV of the participant extracted from the database (ΔV DB)

ID	PARTNR	TYPE	SEGMENT	$\Delta V(\mathrm{DB})[\mathrm{km/h}]$
1	1	Front-Rear	C	23
1	2	Front-Rear	SUV	20
2	1	Front-Side	C	25
2	2	Front-Side	SUV	19
3	1	Sliding	C	16
3	2	Sliding	C	16
4	1	Front-Rear	C	32
4	2	Front-Rear	D	34
5	1	Small Overlap	E	14
5	2	Small Overlap.	C	19
6	1	Small Overlap	SUV	9
6	2	Small Overlap	C	14
7	1	Front-Side	SUV	33
7	2	Front-Side	B	38
8	1	Front-Side	C	21
8	2	Front-Side	B	27
9	1	Front-Side	B	19
9	2	Front-Side	A	23
10	1	Front-Side	D	28
10	2	Front-Side	B	39
11	1	Front-Side	B	22
11	2	Front-Side	SUV	17
12	1	Sliding	B	9
12	2	Sliding	C	7
13	1	Front-Front	B	13
13	2	Front-Front	A	13
14	1	Front-Rear	E	21
14	2	Front-Rear	D	27
15	1	Front-Rear	D	15
15	2	Front-Rear	SUV	11
16	1	Sliding	B	11
16	2	Sliding	C	8
17	1	Front-Side	B	10
17	2	Front-Side	C	9
18	1	Front-Side	A	33
18	2	Front-Side	B	30
19	1	Front-Front	C	23
19	2	Front-Front	C	22
20	1	Front-Side	B	21
20	2	Front-Side	SUV	15

Table A2 Results of the simulations of the 20 real accidents extracted from the IGLAD PCM database. Respectively: accident identifier (ID), participant identifier (PARTNR), ΔV of the participant extracted from the database (ΔV DB), ΔV of the participant simulated with the real shape (ΔV CS), ΔV of the participant simulated with the rectangular shape (ΔV RS), absolute error on ΔV of the participant simulated with the real shape (ΔV error CS), absolute error on ΔV of the participant simulated with the rectangular shape (ΔV error RS), relative error on ΔV of the participant simulated with the real shape (ΔV relative error CS), and relative error on ΔV of the participant simulated with the rectangular shape (ΔV relative error RS)

ID	PARTNR	ΔV [km/h] (DB)	ΔV [km/h] (CS)	ΔV [km/h] (RS)	ΔV error [km/h] (CS)	ΔV error [km/h] (CS)	ΔVrelative error (CS)	ΔV relative error (RS)
1	1	23	23,5	24,8	−0,5	−1,8	−2,2%	−7,7%
1	2	20	20,0	21,2	0,0	−1,2	0,0%	−5,8%
2	1	25	23,3	30,1	1,7	−5,1	6,8%	−20,3%
2	2	19	18,8	24,0	0,2	−5,0	1,1%	−26,3%
3	1	16	16,4	15,2	−0,4	0,9	−2,5%	5,3%
3	2	16	15,6	14,5	0,4	1,5	2,5%	9,4%
4	1	32	28,8	44,7	3,2	−12,7	10,0%	−39,8%
4	2	34	30,8	49,5	3,2	−15,5	9,4%	−45,6%
5	1	14	18,9	19,6	−4,9	−5,6	−35,0%	−40,2%
5	2	19	22,8	23,6	−3,8	−4,6	−20,0 v	−24,4%
6	1	9	13,0	8,1	−4,0	0,9	−44,4%	9,9%
6	2	14	18,7	13,1	−4,7	0,9	−33,6%	6,4%
7	1	33	28,8	31,2	4,2	1,8	12,7%	5,6%
7	2	38	37,8	41,3	0,2	−3,3	0,5%	−8,7%
8	1	21	17,5	22,7	3,5	−1,7	16,7%	−8,0%
8	2	27	24,8	30,0	2,2	−3,0	8,1%	−10,9%
9	1	19	20,2	28,1	−1,2	−9,1	−6,1%	−47,8%
9	2	23	23,9	24,1	−0,9	−1,1	−3,9%	−4,6%
10	1	28	26,1	32,6	1,9	−4,6	6,8%	−16,3%
10	2	39	36,3	44,7	2,7	−5,7	6,9%	−14,6%
11	1	22	23,6	26,8	−1,6	−4,8	−7,3%	−22,0%
11	2	17	17,1	20,5	−0,1	−3,5	−0,6%	−20,4%
12	1	9	12,0	10,1	−3,0	−1,1	−33,3%	−12,3%
12	2	7	5,8	4,6	1,2	2,4	17,1%	33,7%
13	1	13	13,0	17,7	0,0	−4,7	0,0%	−35,9%
13	2	13	13,9	18,6	−0,9	−5,6	−6,9%	−43,4%
14	1	21	22,0	30,6	−1,0	−9,6	−4,8%	−45,6%
14	2	27	25,0	34,8	2,0	−7,8	7,4%	−28,8%
15	1	15	14,4	20,2	0,6	−5,2	4,0%	−34,3%
15	2	11	10,8	15,2	0,2	−4,2	1,8%	−37,9%
16	1	11	7,3	5,4	3,7	5,6	33,6%	50,5%
16	2	8	8,0	8,4	0,0	−0,4	0,0%	−5,1%
17	1	10	9,1	6,1	0,9	3,9	9,0%	38,8%
17	2	9	6,4	5,6	2,6	3,4	28,9%	37,8%
18	1	33	31,1	38,7	1,9	−5,7	5,8%	−17,1%
18	2	30	29,2	36,9	0,8	−6,9	2,7%	−23,0%
19	1	23	18,8	1,4	4,2	21,6	18,3%	94,0%
19	2	22	18,2	2,1	3,8	19,9	17,3%	90,5%
20	1	21	16,1	16,8	4,9	4,2	23,3%	20,1%
20	2	15	10,1	10,7	4,9	4,4	32,7%	29,0%

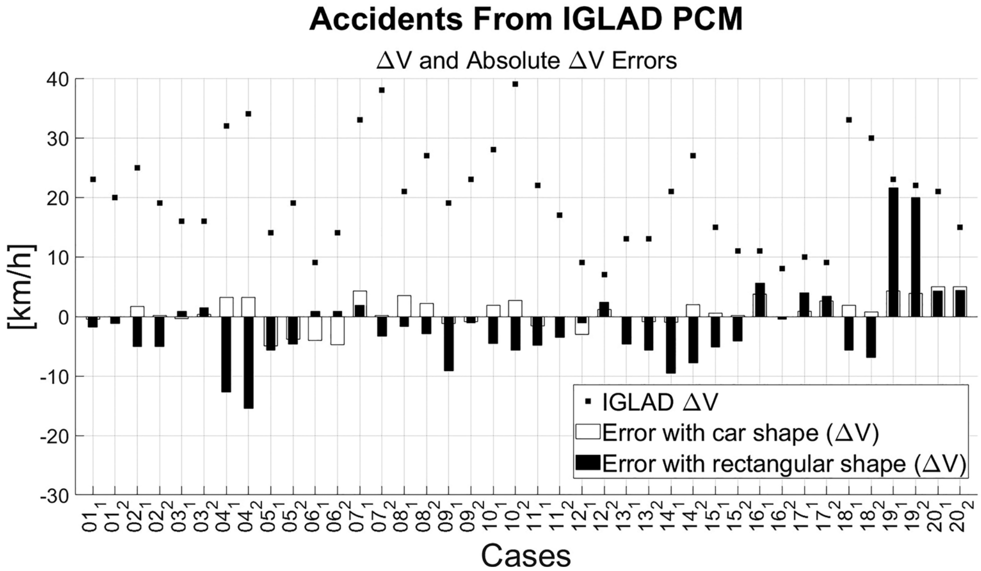

Fig. A8 Errors on ΔV obtained by simulating the vehicles with real shapes (in white) and with rectangular shapes (in black), expressed relative to the values reconstructed and encoded in the IGLAD PCM database. Subscripts distinguish between participant 1 and participant 2 in the same accident. The ΔV value recorded in the database for each participant is also reported

Table A3 Results of the simulations of the 20 real accidents extracted from the IGLAD PCM database. Respectively: accident identifier (ID), participant identifier (PARTNR), IR of the participant extracted from the database (IR DB), IR of the participant simulated with the real shape (IR CS), IR of the participant simulated with the rectangular shape (IR RS), absolute error on IR of the participant simulated with the real shape (IR error CS), and absolute error on IR of the participant simulated with the rectangular shape (IR error RS)

ID	PARTNR	IR (DB)	IR (CS)	IR (RS)	IR error (CS)	IR error (RS)
1	1	4,0%	4,4%	5,4%	−0,4%	−1,4%
1	2	0,9%	0,9%	1,1%	0,0%	−0,2%
2	1	11,9%	8,8%	27,2%	3,1%	−15,2%
2	2	2,0%	2,0%	4,7%	0,1%	−2,7%
3	1	0,5%	0,5%	0,4%	0,0%	0,1%
3	2	1,2%	1,1%	0,9%	0,1%	0,3%
4	1	5,2%	3,3%	27,1%	1,9%	−21,9%
4	2	22,3%	14,1%	81,2%	8,2%	−58,9%
5	1	0,9%	2,0%	2,3%	−1,1%	−1,4%
5	2	0,8%	1,4%	1,5%	−0,6%	−0,8%
6	1	0,4%	0,7%	0,3%	−0,4%	0,1%
6	2	0,9%	1,9%	0,7%	−1,1%	0,1%
7	1	19,4%	10,3%	14,8%	9,0%	4,5%
7	2	64,6%	63,6%	77,9%	0,9%	−13,3%
8	1	5,7%	2,9%	7,9%	2,8%	−2,1%
8	2	7,8%	5,4%	12,4%	2,3%	−4,6%
9	1	2,0%	2,5%	9,2%	−0,4%	−7,2%
9	2	8,3%	9,8%	10,1%	−1,5%	−1,7%
10	1	19,8%	14,4%	38,0%	5,4%	−18,2%
10	2	40,7%	30,0%	65,0%	10,7%	−24,3%
11	1	3,4%	4,4%	7,6%	−1,0%	−4,2%
11	2	4,9%	5,0%	10,0%	−0,1%	−5,2%
12	1	0,5%	1,0%	0,7%	−0,4%	−0,1%
12	2	0,4%	0,3%	0,2%	0,1%	0,1%
13	1	0,7%	0,7%	1,6%	0,0%	−0,9%
13	2	0,7%	0,8%	1,9%	−0,1%	−1,2%
14	1	2,9%	3,4%	13,6%	−0,5%	−10,7%
14	2	2,5%	1,9%	7,7%	0,6%	−5,2%

Table A3 (continued)

ID	PARTNR	IR (DB)	IR (CS)	IR (RS)	IR error (CS)	IR error (RS)
15	1	1,0%	0,9%	2,5%	0,1%	−1,5%
15	2	0,2%	0,2%	0,4%	0,0%	−0,2%
16	1	0,5%	0,3%	0,2%	0,2%	0,3%
16	2	0,7%	0,7%	0,7%	0,0%	−0,1%
17	1	0,4%	0,4%	0,2%	0,1%	0,2%
17	2	0,5%	0,3%	0,3%	0,2%	0,3%
18	1	40,1%	31,4%	67,5%	8,7%	−27,3%
18	2	12,5%	11,0%	32,2%	1,4%	−19,8%
19	1	4,0%	2,0%	0,1%	2,0%	3,9%
19	2	3,4%	1,8%	0,1%	1,6%	3,3%
20	1	2,9%	1,2%	1,4%	1,6%	1,5%
20	2	1,8%	0,7%	0,8%	1,1%	1,0%

Author contributions M.-S. G., G. V., and D. V. contributed to the study conception and design. Material preparation, data collection, and analysis were performed by M-S. G., G. V., and G. A., The first draft of the manuscript was written by G. V., M.-S. G., G. V. and D. V. reviewed and edited the manuscript, and D. V. provided supervision and project administration. All authors read and approved the final manuscript.

Funding Not applicable.

Data availability The data that support the findings of this study are available from the corresponding author upon reasonable request.

Declarations

Competing interests The authors declare no competing interests.

References

Alvarez S, Page Y, Sander U, Fahrenkrog F, Helmer T, Jung O, Hermitte T, Düering M, Döering S, Camp O (2017) Prospective effectiveness assessment of adas and active safety systems via virtual simulation: a review of the current practices. In 25th International Technical Conference on the Enhanced Safety of Vehicles (ESV), National Highway Traffic Safety Administration

Bieker G, Tietge U, Rodriguez F, Mock P (2019 Dec) European vehicle market statistics: pocketbook 2019/20. Technical report, International Council on clean Transportation (ICCT). https://theicct.org/sites/default/files/publications/European_vehicle_market_statistics_20192020_20191216.pdf. Accessed 19 Aug 2025

Brach RM (1983) Analysis of planar vehicle collisions using equations of impulse and momentum. Accident Anal Prev 15(2):105–120. https://doi.org/10.1016/0001-4575(83)90067-2

Breitlauch P, Erbsmehl CT, Ratingen M, Mallada JL, Sandner V, Ferson N, Urban M (2023) A novel method for the automated simulation of various vehicle collisions to estimate crash severity. Traffic Inj Prev 24(sup1):S116–S123. https://doi.org/10.1080/15389588.2022.2159761

Campbell K (1974) Energy as a basis for accident severity. SAE Paper 74056

Canadian Council of Motor Transport Administrators (2016) Canada's road safety strategy 2025. https://towardszero.nsw.gov.au/sites/default/files/2024-07/TNSW10046-Road-Safety-Action-Plan-2026_1_0.pdf

Costa C, Gaewsky JP, Stitzel JD, Gayzik FS, Hsu F-C, Martin RS, Miller AN, Weaver AA (2022) Development and implementation of a time- and computationally-efficient methodology for reconstructing real-world crashes using finite element modeling to improve crash injury research investigations. Comput Methods Biomech Biomed Eng 25(12):1332–1349. https://doi.org/10.1080/10255842.2021.2009469

European Climate Infrastructure and Environment Executive Agency (2022) EU road safety: towards 'vision zero'. https://cinea.ec.europa.eu/publications/eu-road-safety-towards-vision-zero_en

European Commission (2003) European road safety action programme – halving the number of road accident victims in the European Union by 2010: a shared responsibility. Publications Office of the European Union, Brussels. https://op.europa.eu/en/publication-detail/-/publication/c8918190-cc5e-4dad-84b5-6199544e08c5. Accessed 18 Aug 2025

European Parliament and Council of the European Union (2007) Directive 2007/46/EC of 5 September 2007 establishing a framework for the approval of motor vehicles and their trailers, and of systems, components and separate technical units intended for such vehicles (framework directive). Official journal of the European Union, L 263. https://eur-lex.europa.eu/legal-content/EN/ALL/?uri=CELEX:32007L0046. Accessed 19 Aug 2025

General Authority for Roads, Ministry of Transport and Logistic Services, Saudi Arabia (2025) Road code: 25 regulations for road planning, maintenance and safety. https://saudipress.com/saudi-arabia-introduces-comprehensive-road-safety-regulations. Accessed 18 Aug 2025

Gotoh E, Ohsawa S, Satoh Y, Yasuda S (1992) An investigation of steering column collapse behavior using finite element analysis. Technical Paper 920391, SAE International. https://doi.org/10.4271/920391

Gulino M-S, Sortino A, Vangi D (2025) The effect of pre-crash variables on occupants' injury risk in car impacts: assessment by

feature ranking, regression, and machine learning for increasing injury scales. Eur Transp Res Rev 17(1):40. https://doi.org/10.1186/s12544-025-00736-7
Gulino M-S, Vichi G, Vangi D (2025) Validation of a virtual forward simulation tool for adas assessment. Eur Transp Res Rev 17(1):1–29. https://doi.org/10.1186/s12544-025-00724-x
Gulino MS, Fiorentino A, Vangi D (2022) Prospective and retrospective performance assessment of advanced driver assistance systems in imminent collision scenarios: the cmi-v r approach. Eur Transp Res Rev 14(1):3. https://doi.org/10.1186/s12544-022-00527-4
Hamza K, Saitou K (2005) Design optimization of vehicle structures for Crashworthiness using equivalent mechanism approximations. J Mech Des 127(3):485–492. https://doi.org/10.1115/1.1862680. https://asmedigitalcollection.asme.org/mechanicaldesign/article-pdf/127/3/485/5601657/485_1.pdf
Hu S, Lü X, Zhang X, Zhang H, Hong D, Zhou D (2020) Design and verification of pedestrian protection airbag. Automot Eng 42(5):608–614. https://doi.org/10.19562/j.chinasae.qcgc.2020.05.007
Imprialou M, Quddus M (2019) Crash data quality for road safety research: current state and future directions. Accident Anal Prev 130:84–90. https://doi.org/10.1016/j.aap.2017.02.022
Ishikawa H (1993) Impact model for accident reconstruction-normal and tangential restitution coefficients. Technical report, SAE Technical Paper
Jurewicz C, Sobhani A, Woolley J, Dutschke J, Corben B (2016) Exploration of vehicle impact speed – injury severity relationships for application in safer road design. Transp Res Procedia 14:4247–4256. https://doi.org/10.1016/j.trpro.2016.05.396. Transport Research Arena TRA2016
Kolk H, Tomasch E, Sinz W, Bakker J, Dobberstein J (2017). Evaluation of a momentum based impact model and application in an effectivity study considering junction accidents
Kubiak P (2017) Nonlinear approximation method of vehicle velocity vt and statistical population of experimental cases. Forensic Sci Int 281:147–151. https://doi.org/10.1016/j.forsciint.2017.10.032
Le Guennec Y, Brunet J-P, Daim F-Z, Chau M, Tourbier Y (2018) A parametric and non-intrusive reduced order model of car crash simulation. Comput Methods Appl Mech Eng 338:186–207. https://doi.org/10.1016/j.cma.2018.03.005
Li G, Lyons M, Wang B, Yang J, Otte D, Simms C (2017) The influence of passenger car front shape on pedestrian injury risk observed from German in-depth accident data. Accident Anal Prev 101:11–21. https://doi.org/10.1016/j.aap.2017.01.012
McHenry RR, McHenry BG (1997) Effects of restitution in the application of crush coefficients. SAE Trans 1696–1716
National Traffic Safety Committee & Qatar Transportation and Traffic Safety Center (2012) Qatar National road safety strategy 2012–2022. https://www.roadsafety.qa/about-us/. Accessed: 18 Aug 2025
Organisation for Economic Co-operation and Development (2016) Road safety country profiles. https://www.itf-oecd.org/sites/default/files/japan-road-safety.pdf
Page Y, Fahrenkrog F, Fiorentino A, Gwehenberger J, Helmer T, Lindman M, Camp O, Sander U, Puch S, Wimmer P (2015) A comprehensive and harmonized method for assessing the effectiveness of advanced driver assistance systems by virtual simulation: the p.e.a.r.s. initiative. Accident Anal Prev). Accessed 18 Aug 2025
Pahlavani M, Marzbanrad J (2015) Crashworthiness study of a full vehicle-lumped model using parameters optimisation. Int J Crashworthiness 20(6):573–591. https://doi.org/10.1080/13588265.2015.1068910
Roads & Transport Authority (RTA), Dubai (2021) Dubai Traffic safety strategy. https://u.ae/en/information-and-services/justice-safety-and-the-law/road-safety/road-safety-initiatives. Accessed 18 Aug 2025
Roberts VL, Compton CP (1993) The relationship between delta v and injury. Technical report, SAE Technical Paper
Sander U, Lubbe N (2018) Market penetration of intersection aeb: characterizing avoided and residual straight crossing path accidents. Accident Anal Prev 115:178–188. https://doi.org/10.1016/j.aap.2018.03.025
Schubert A, Liers H, Petzold M (2017) The gidas pre-crash-matrix 2016. innovations for standardized pre-crash-scenarios on the basis of the vufo simulation model vast. Berichte der bundesanstalt fuer Strassenwesen. Unterreihe Fahrzeugtechnik 117
Shaikh J, Sander U (2018) Creation of pre-crash time-series database for evaluation of active safety systems using rassi data. In 8th International Conference on ESAR "Expert Symposium on Accident Research, Hanover, Germany
Shaikh J, Sui B, Lubbe N (2024) Creation of pre-crash time-series data using Chinese in-depth crash database from shufo. In Proceedings of the IRCOBI Conference 2024, pp 1111–1130). IRC-24-130
Smit S, Tomasch E, Kolk H, Plank MA, Gugler J, Glaser H (2019) Evaluation of a momentum based impact model in frontal car collisions for the prospective assessment of adas. Eur Transp Res Rev 11(1):1–9. https://doi.org/10.1186/s12544-018-0343-3
Spitzhüttl F, Liers H, Petzold M (2015) Creation of pre-crash simulations in global traffic accident scenarios based on the iglad database. In Proceedings of Future Active Safety Technology Towards zero traffic accidents (FASTzero), pp 427–433
Taichi Shiiba T, Fehr J, Eberhard P (2012) Flexible multibody simulation of automotive systems with non-modal model reduction techniques. Vehicle System Dyn 50(12):1905–1922. https://doi.org/10.1080/00423114.2012.700403
Tan H, Zhao F, Hao H, Liu Z (2020) Estimate of safety impact of lane keeping assistant system on fatalities and injuries reduction for China: scenarios through 2030. Traffic Inj Prev 21(2):156–162. https://doi.org/10.1080/15389588.2020.1711518
Terranova P, Guo F, Perez MA (2026) Evaluating risk factors associated with fatalities among powered two-wheeler crashes in the United States. Traffic Inj Prev 27(2):172–179. https://doi.org/10.1080/15389588.2025.2494235
Transport for NSW (2022) 2026 road safety action plan. https://towardszero.nsw.gov.au/sites/default/files/2024-07/TNSW10046-Road-Safety-Action-Plan-2026_1_0.pdf
Vangi D, Begani F, Spitzhüttl F, Gulino M-S (2019) Vehicle accident reconstruction by a reduced order impact model. Forensic Sci Int 298:e426.1–.e426.11. https://doi.org/10.1016/j.forsciint.2019.02.042
Vangi D, Gulino M-S, Cialdai C (2019) Coherence assessment of accident database kinematic data. Accident Anal Prev 123:356–364. https://doi.org/10.1016/j.aap.2018.12.004
Witold Pawlus W, Reza H, Robbersmyr KG (2011) Application of viscoelastic hybrid models to vehicle crash simulation. Int J Crashworthiness 16(2):195–205. https://doi.org/10.1080/13588265.2011.553362
World Health Organization (2023) Global status report on road safety 2023. World Health Organization
Xiao Z, Wang L, Mo F, Lv X, Yang C (2020) Influences of impact scenarios and vehicle front-end design on head injury risk of motorcyclist. Accident Anal Prev 145:105697. https://doi.org/10.1016/j.aap.2020.105697